*CHAPTER 7*

# STUDY ON (Dy AND Co) DOPED ZnO THIN FILM FOR ULTRAVIOLET PHOTODETECTOR APPLICATION BY SOL GEL SPIN COATING TECHNIQUE

## 7.1. INTRODUCTION

This chapter explains the preparation and characterisation of pure and doped Zinc oxide thin films for UV detector application. This chapter deals with study of Dy doped ZnO thin film for UV detector application and explains the structural and optical properties of Co doped ZnO thin film. ZnO is an II-VI compound semiconductor with stable wurtzite structure. ZnO has been considered as a potential material, compare to other wide bandgap semiconductors, for ultraviolet (UV) photodetector applications due to its unique properties and easy processing. Recently, doping of lanthanide elements in ZnO makes its promising candidate for wide range applications [201]. However, photoconductivity of ZnO thin films depends on preparation condition, surface morphology, and defects in the thin film. The properties of photodetector are strongly influenced by presence of defects and grain boundaries. The scientific fraternity have put a lot of effort to control the defects in the system via doping of foreign elements. Recently, the ultra-thin layer of metals with ZnO is fabricated for UV detector with enhanced photoconductivity using controlled surface defects by providing extra electrons [202]. We have tried to control these defects by doping of rare earth materials and transition metal in ZnO.

**Study on Dy Doped ZnO Thin Film**

The lanthanide materials exhibit luminescence in visible region due to intra shell f-f transition. Among all rare earth materials, Dy doped ZnO has attracted much attention of scientific fraternity due to its unique luminescence properties, which is useful in flat

panel display and white light emitting diode etc. $Dy^{+3}$ ions exhibit emission in yellow and blue, which can be attributed to $^4F_{9/2} \rightarrow {}^6H_{13/2}$ and $^4F_{9/2} \rightarrow {}^6H_{15/2}$ transitions [203]. The intensity of yellow emission is very sensitive to the environment and depends on the host. The proper engineering of yellow/blue ratio leads to solid-state lighting application. Recently, *Hastir et. al.* reported the doping of rare earth materials (Dy, Tb, and Er) in ZnO for sensor applications [178]. The rare earth materials have been used as a dopant to enhance the sensing properties of ZnO. It has been observed that rare earth doping significantly affect surface basicity, increases surface area and concentration of oxygen vacancies, due to which it has better sensing response for ethanol and acetone detection as compared to pure ZnO sensor [178]. By using these rare earth materials, there is an urgent need to check the photodetector applications. The UV photodetector with high detectivity and fast response are required for flame sensing, UV photography, air quality monitoring, and satellite-based missile plum detection etc. It is well known that surface morphology and defects depend on the synthesis process of the film. ZnO thin films can be prepared by different techniques, such as pulse laser deposition, thermal evaporation, chemical vapour deposition and sol-gel spin coating method. Among all preparation method, the sol-gel spin coating process is better due to easy control of chemical components, precise control on the thickness of the film, and fabrication of smooth surface thin film at low cost.

In this work, we have investigated (possibly first time) properties of Dy doped ZnO for its application in UV light detection. We have prepared Dy(1%) doped ZnO thin film with the help of sol-gel spin coating technique. The prepared sample has been characterized to confirm structural property, surface morphology and its feasibility as a UV detector. The enhancement in UV region absorption, increase in responsivity and

photocurrent indicate that Dy doped ZnO thin film can be a promising candidate for UV detector.

## 7.2. EXPERIMENTAL PROCEDURE

### 7.2.1 Synthesis of ZnO and Doped ZnO Thin Films

Thin films of ZnO and Dy (1%) doped ZnO have been prepared on the glass substrate with the help of sol-gel spin coating technique. The starting materials were zinc acetate dehydrates and dysprosium (III) acetate tetrahydrates. Monoethanolamine (MEA) and ethanol were used as a stabilizer and solvent, respectively. Briefly, for Dy (1%) doped ZnO thin film preparation, we take the stoichiometric amount of zinc acetate dehydrate and dissolve it into ethanol and start stirring at 1200 rpm for two hours. After that, the stoichiometric amount of dysprosium (III) acetate tetrahydrates was added, and stirring was done continuously two hours for complete dissolution of the precursor. The small amount of MEA has been added to the solution to get the clear transparent solution of 0.3M concentration and stirring was started for three hours to get a solution for Dy doped ZnO thin film preparation. The glass substrates were properly cleaned with alkenox detergent and DI water followed by acetone and propanol for 10 min each in the ultrasonic cleaner. The substrates were preheated in an oven at 200°C for 10 min to remove all the impurities from the surface of the substrate. The speed of spin coater was maintained at 3000 rpm for one min. at room temperature. After deposition of each layer, the samples were heated in hot air oven at 200°C for 10 min to remove organic residuals and evaporate the solvent. These procedures of coating and drying have been repeated four times to prepare a sample. The obtained film was annealed in air at 550°C for one hour. Similar techniques have been employed to prepare Co doped ZnO thin film. The final sample obtained after annealing has been used for morphology, structural, optical,

and other characterizations. The high purity Ag (99.99%) was used to prepare contact by thermal evaporation (FL400 HHV) method for electrical property measurement.

### 7.2.2 Characterizations

Phase confirmation and nature of crystallinity of thin film samples were measured using High - Resolution X-ray diffraction (Rigaku) with monochromatic Cu-$K_\alpha$ radiation ($\lambda$= 1.54 Å) at inclination angle 1°. All the patterns were recorded over the range of 20° ≤ $2\theta \leq 90°$ with a step size of 0.02°. Atomic Force Microscopy (AFM) NT-MDT setup was employed to analyze the surface morphology of the thin films. Current-Voltage measurements of ZnO and ZnO:Dy(1%) films were performed using a source meter (Keithley, 2410) setup. UV lamp of wavelength of 325 nm was used. The optical absorption spectra of the thin film samples were recorded in the range of 200-800nm by Jasco-V770 spectrophotometer. Photoluminescence spectra have been measured by Horiba Fluorolog-3 spectrophotometer equipped with 450w Xe flash lamp.

## 7.3. RESULTS AND DISCUSSION OF Dy DOPED ZnO THIN FILM

### 7.3.1. Structural Analysis

Before electrical characterizations, structural and morphology of ZnO and ZnO:Dy(1%) thin films have been investigated. The crystalline structure and purity of the films have been analyzed by HR-XRD measurement. Figure 7.1 depicts the HR-XRD pattern of ZnO and Dy doped ZnO thin film in the range of 20°-90°. The sharp peaks ascertain the crystalline nature of the samples. All observed HR-XRD peaks are properly indexed according to standard Bragg's position of hexagonal wurtzite ZnO (PDF#792205). We could not find any impurity peak within the detection limit of the instrument. The most intense peak at 2θ= 34.29° belongs to (002) plane oriented along *c*-axis of wurtzite structure of ZnO thin film. The decrease in HR-XRD peak intensity in ZnO:Dy(1%) indicates small lattice distortion due to the presence of Dy. In fact, after

doping of Dy in ZnO matrix, Zn is replaced by Dy. The lattice distortion arises due to the difference in ionic radii of $Zn^{+2}$ ions (0.74Å) and $Dy^{+3}$ ions (0.91Å)[204]. The unit cell volume has been estimated using Equation 4.1. The calculated values of the unit cell volume are listed in Table 7.1. Atomic packing fraction (APF) of the samples has been calculated using relation 4.2. The values of APF are listed in Table 7.1. It can be pointed out that unit cell volume and APF of Dy doped ZnO thin film is slightly greater than pure ZnO. This may be due to decrement in the voids. The observed variation in unit cell volume and APF can be attributed to effect of Dy dopant, which influences the lattice parameter. The observed value of APF (approximately 75%) is slightly greater than APF of bulk ZnO (74%). The small increase may be due to the size effect. The crystallite size of the samples has been calculated by Scherer's formula [205] (Equation 3.1).

The calculated values of crystallite size for ZnO and Dy doped ZnO thin films are 17 nm and 15 nm, respectively. The crystallite is controlled by grain growth in the film and grain growth in ZnO depends on moment and diffusion of $Zn^{+2}$ ions in the system. Since the ionic radius of $Dy^{+3}$ (0.91 Å) is greater than $Zn^{+2}$ (0.74 Å), therefore the presence of Dy in the lattice restrain the grain growth; as a result crystallite size is reduces for Dy doped ZnO. *Ajimsha et al.* have reported the effect of Dy doping and shown the same trend in crystallite size due to Dy doping [206]. We have observed that lattice parameter '*a*' increases after Dy doping in ZnO. The values of lattice parameters are listed in Table 7.1. The observed increase in lattice parameter can be attributed to lattice expansion due to Dy doping. The substitution of Dy (0.91Å) at the host cation place will lead to lattice expansion due to Dy-O-Zn type bond formation. The decrease in the intensity of (002) XRD peak (Figure 7.1) of Dy doped ZnO thin film indicates that sample is not preferably oriented along *c*-axis and texture property decreases due to Dy doping. In addition, some small intensity peaks [(102), (103)] in Dy doped ZnO are disappeared due to change in

crystalline quality. The small decrease in lattice parameter '*c*' occurs to maintain the crystal structure of the host, which is indicated by less intense (002) peak.

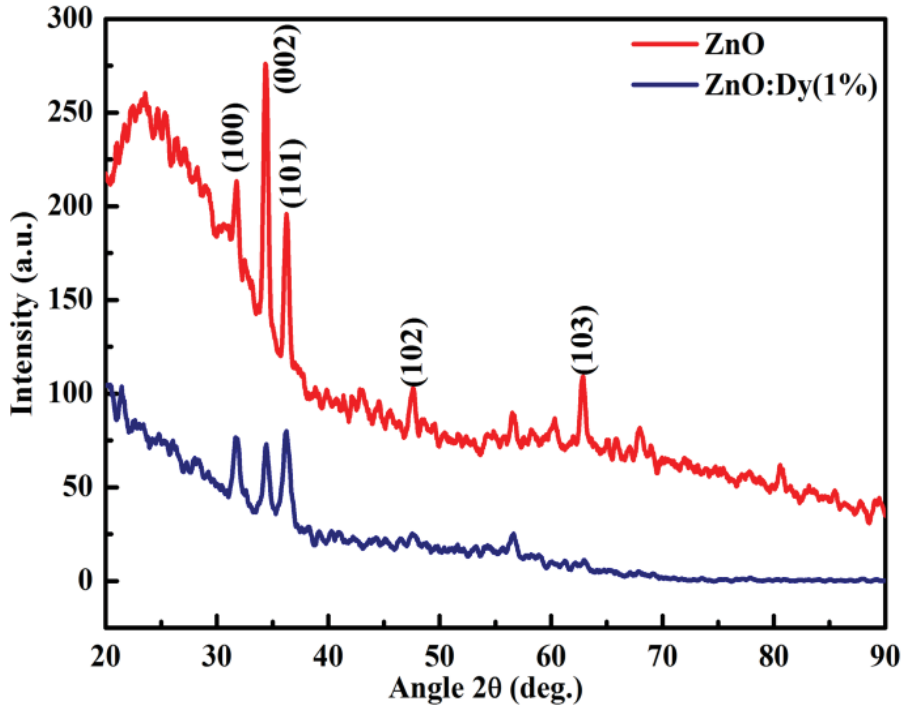


**Figure 7.1:** HR-XRD spectra of pure and Dy doped ZnO thin film.

**Table 7.1**. The lattice parameter, crystallite size, unit cell volume and APF of the samples.

| Composition | Lattice parameter | | Crystallite size (nm) | Cell volume $(Å)^3$ | APF |
|---|---|---|---|---|---|
| | a(Å) | c(Å) | | | |
| ZnO | 3.2466 | 5.2112 | 17 | 47.5711 | 0.7529 |
| ZnO: Dy(1%) | 3.2494 | 5.2026 | 15 | 47.5722 | 0.7548 |

### 7.3.2 Surface Morphology

The surface morphology of thin films has been investigated by Atomic Force Microscopy (AFM). The morphology of ZnO and Dy doped ZnO thin films have granular nature. Figure 7.2(a) and (b) depicts 2D AFM image of ZnO and Dy doped ZnO thin films. The AFM image indicates a dense distribution of grains with well-defined grain boundaries. The grain size distribution of ZnO and Dy doped thin film is shown in the

inset of Figure 7.2(a) and 7.2(b) respectively. The grain size analysis has been carried out with the help of Nova Px software. The average grain size of ZnO and ZnO:Dy(1%) has been estimated by Gaussian fitting of grain size distribution and found to be 51 and 66 nm respectively. The observed result indicates that grain size increases with Dy doping in ZnO. The maximum particles in ZnO thin film lie in the range of 40-60 nm, while Dy doped ZnO have the maximum particle in 10-30nm range. The observed grain size decreases with Dy doping and supports the nature of crystallite size variation. The average roughness of ZnO and Dy doped ZnO thin films are 5.3 nm and 5.5 nm, respectively. The observed value of roughness indicates smooth surface morphology of the thin films. The small increase in roughness value is due to substitution of higher ionic radius element (Dy) in the system.

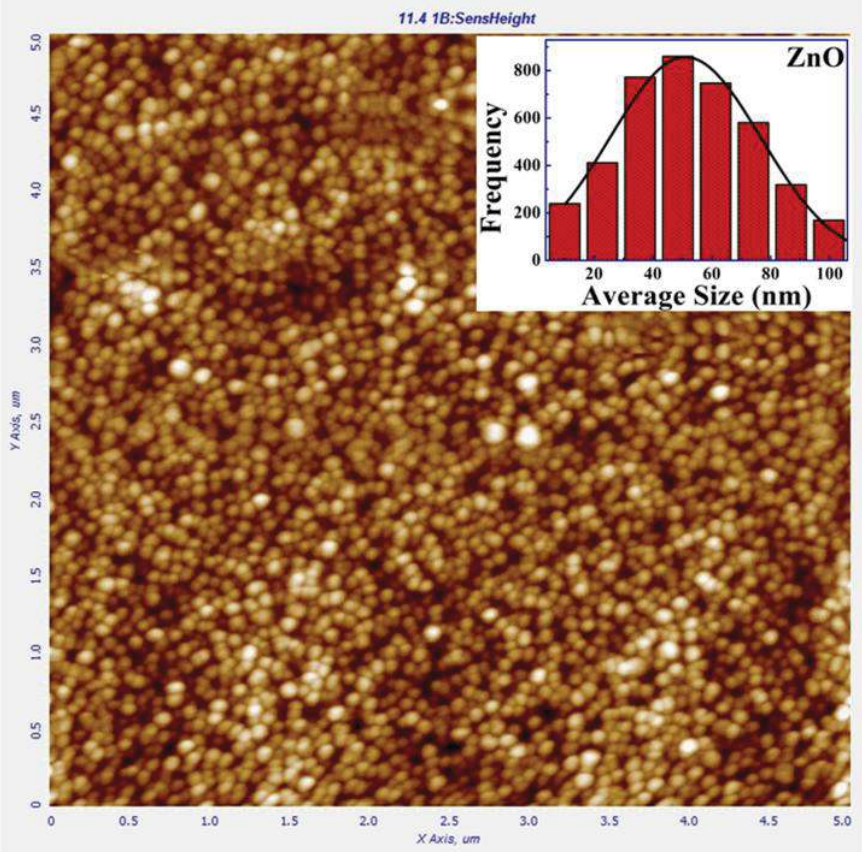


**Figure 7.2(a):** 2D AFM image of ZnO thin film. The inset shows grain size distribution.

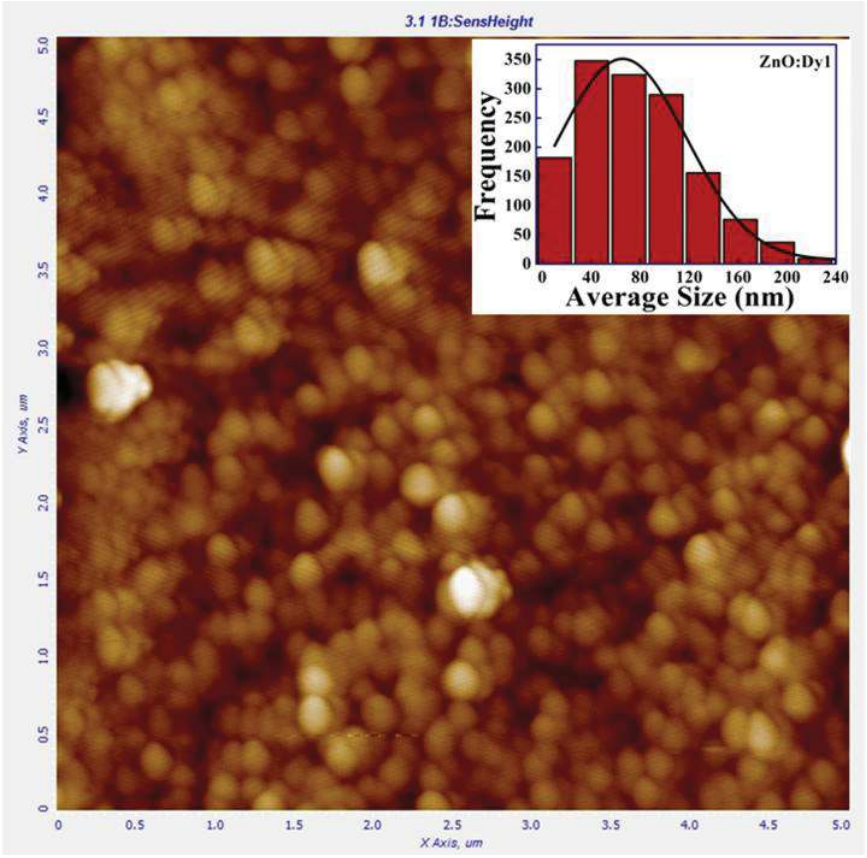


**Figure 7.2(b):** 2D AFM image of ZnO:Dy(1%) thin film. The inset shows grain size distribution.

### 7.3.3 Absorption Analysis

It is well known that crystalline structure and surface morphology play an important role in optical properties. Figure 7.3 shows the absorption spectra of the ZnO, and Dy doped ZnO films in the wavelength range of 200 nm-800 nm. The spectra confirm that ZnO and Dy doped ZnO films show strong absorption in the wavelength range of 300 nm-400 nm. The intensity of absorption spectra increases significantly in Dy doped ZnO thin film than ZnO film. This indicates the high sensitivity of Dy1 in 300-370 nm range as compared to pure ZnO thin film. The well-known mechanism for UV sensing involves atmospheric oxygen. The ionized atmospheric oxygen on the surface enhances the UV sensing [207-208]. It has been found that Zn vacancies are also responsible for UV

sensing property of ZnO [209]. The substitution of $Dy^{+3}$ at $Zn^{+2}$ site of ZnO crystal structure enhance the defect (Zn vacancies, oxygen vacancies) in the system. Thus the absorption in the UV region increases. The increased in absorption intensity demonstrate the potentiality of the Dy doped ZnO thin film for UV detection applications. The thin film samples shows strong absorption for photon having wavelength less than 370 nm and it is transparent for photon of wavelength greater than 370 nm. The band gap of thin films has been calculated using Tauc relation (Equation 3.2). Tauc plot for ZnO thin film is shown in the inset of Figure 7.3. The value of band gap for both samples is 3.28eV. The band edge at same wavelength maintains the same band gap value for pure and doped thin film samples.

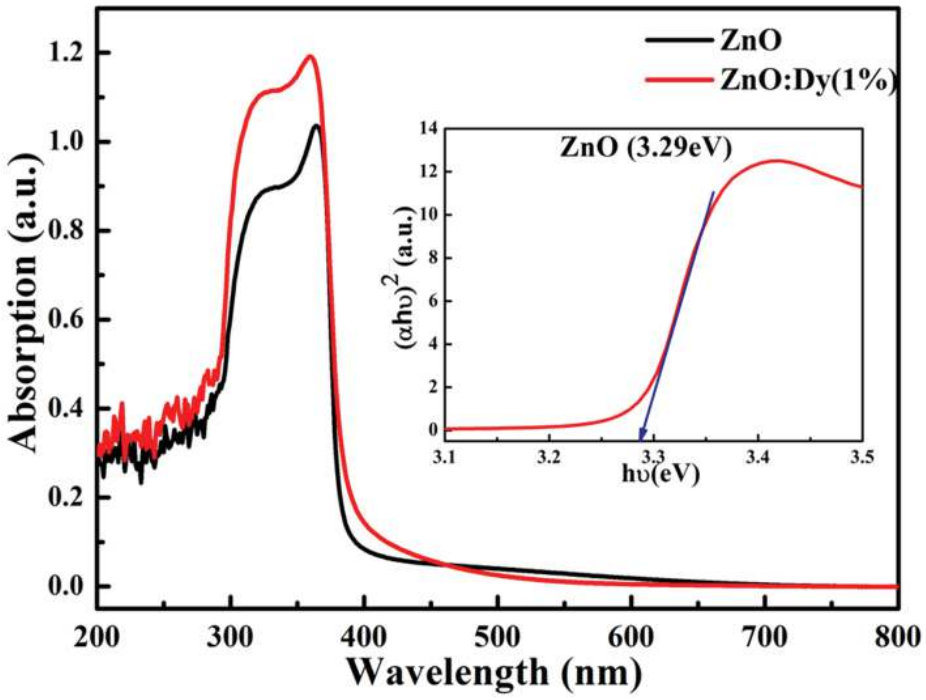


**Figure 7.3:** Absorption spectra of pure and doped ZnO thin film. The inset shows Tauc plot of ZnO thin film.

### 7.3.4 Electrical Analysis

The device structure used for electrical analysis is shown in Figure 7.4. The current-voltage (I-V) characteristics of ZnO and ZnO:Dy(1%) have measured under dark

and UV illumination (λ=325nm) conditions as shown in Figure 7.5(a) and (b) respectively. After UV illumination, an increment in the photocurrent was observed for both samples. The enhancement in the photocurrent (after UV light) was observed from 3.39 μA amp to 105.54 μA at 4.5 V bias for ZnO and ZnO:Dy(1%), respectively. The photocurrent of Dy doped ZnO significantly enhances with the factor of 31 as compared to pristine ZnO at the same bias voltage. This enhancement is due to doping of Dy in ZnO which will absorb more light in UV region as confirmed by absorption spectra shown in Figure 7.3(a). In addition, the rectification ratio for both configurations is calculated by dividing forward to reverse biased current corresponding to 1 V. The rectification ratio is 7.43 for ZnO with UV exposure while for ZnO:Dy(1%), it is 7.76 with UV exposure. Since, It is known that the charge collection and separation efficiencies depend on the rectification ratio and hence, it is also expected that ZnO:Dy(1%) should show good photodetection for UV light. However, it is interesting to note that photoresponse is getting improved after doping of Dy in ZnO (Figure 7.5 (b)) which in turn make it more useful to design a photodetector based on ZnO.

In order to measure temporal response, both the configurations are exposed to pulsed-UV light (λ=325 nm) under 2 V bias condition as shown in Figure 7.5(c) and (d). After Dy doping, a large enhancement is observed in the photocurrent for ZnO:Dy(1%) as compared to pristine ZnO which could be attributed to the local electric field created at the junction by absorbing more light due to Dy doping in ZnO. The photoresponse for both the configurations is calculated by the ratio of on to off currents. It is interesting to note that the photoresponse is getting improved with Dy doping in ZnO which confirms its importance for the photodetector. In fact, Dy helps to absorb more photons and thus, shows an enhancement in the photoresponse as confirmed by absorbance spectra [Figure 7.3].

The responsivity of detector can be defined as [210]

$$R\ (A/W) = \frac{I_p}{P_{opt}}$$

Where $I_p$ is photocurrent and $P_{opt}$ represent incident optical power. The calculated value of responsivity at 4.5 V is 0.032 A/W and 1.01 A/W for ZnO and ZnO:Dy(1%), respectively. The calculated values indicate that doping of Dy in ZnO can enhance responsivity at same bias. The high value of responsivity suggests that Dy doped ZnO can be used for UV detector applications. The observed value of responsivity is comparatively high as compared to some reported value for ZnO based UV detector [211-212] When UV-light is illuminated on ZnO thin film, the electron excited from the valence band to conduction band and become a free exciton [213]. The electrical conductivity of ZnO thin film increases after Dy doping. The incorporation of Dy ions improves the conductivity as well as shows stronger absorption in UV region and contributes more exciton in ZnO. The response time is another important parameter for the photodetector. It can be observed from the Figure 7.5(c) and (d) that photocurrent of ZnO and ZnO:Dy(1%) increases immediately in turn on the light and decreases very fast when UV light was turned off. Figure 7.5(c) and (d) are used to find out the rise time ($\tau_r$) and fall time ($\tau_f$). The $\tau_r$ and $\tau_f$ are defined as a time taken by the device to increase its photocurrent value from 10 % (90 %) to 90 % (10 %) of the peak value. The calculated $\tau_r$ and $\tau_f$ are found to be 6.55 sec and 6.94 sec for ZnO and 6.53 sec and 7.11 sec for ZnO: Dy(1%), respectively. It is known that due to the presence of deep trap states and other defects the charge carrier takes more time to relax and thus, $\tau_f$ is found to be higher in comparison to $\tau_r$ [214]. The observed value of rise time indicates that the proposed Dy doped ZnO photodetector exhibits an appreciative response time, i.e. it could respond to the incident UV light within 6.53 sec. To the best of our knowledge, this is the first report

based on Dy doped ZnO photodetector which exhibits enhanced photoresponse at UV wavelength.

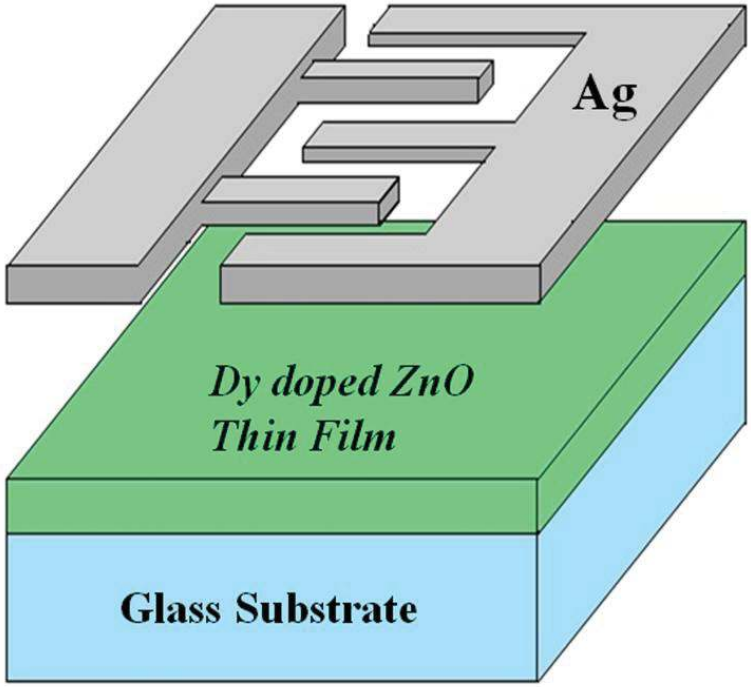


**Figure 7.4:** Device structure fabricated on glass substrate.

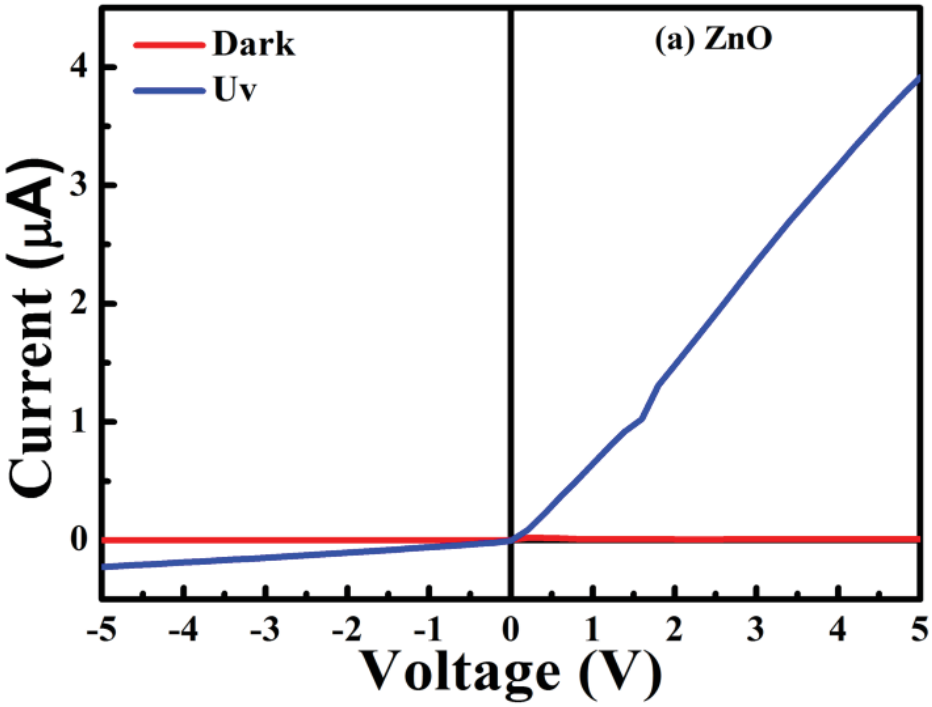


**Figure 7.5(a):** Current-Voltage curve of ZnO.

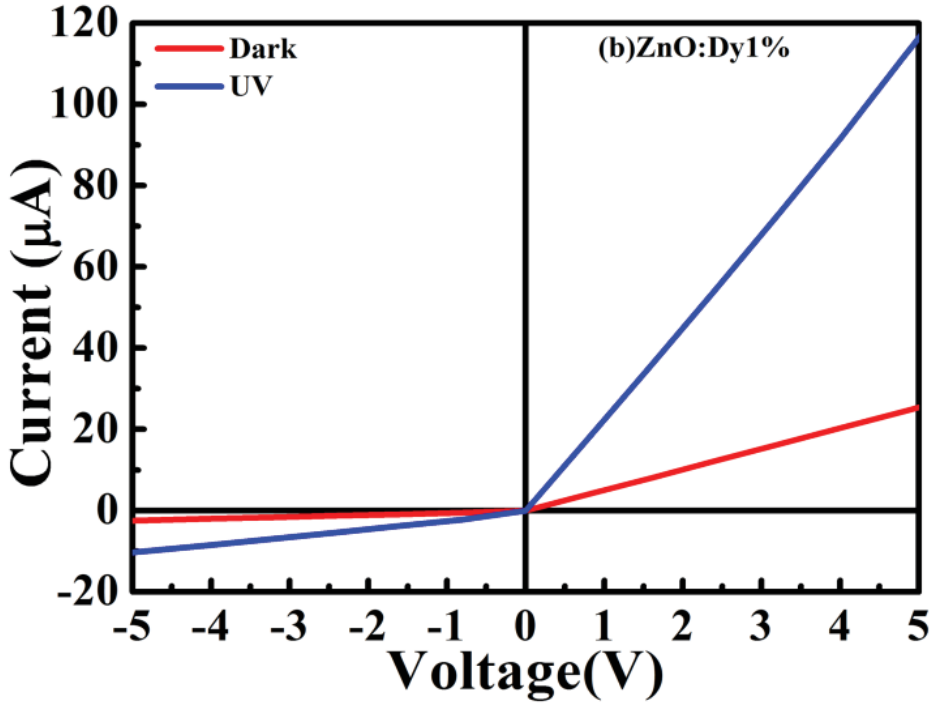


**Figure 7.5(b):** Current-Voltage curve of Dy doped ZnO.

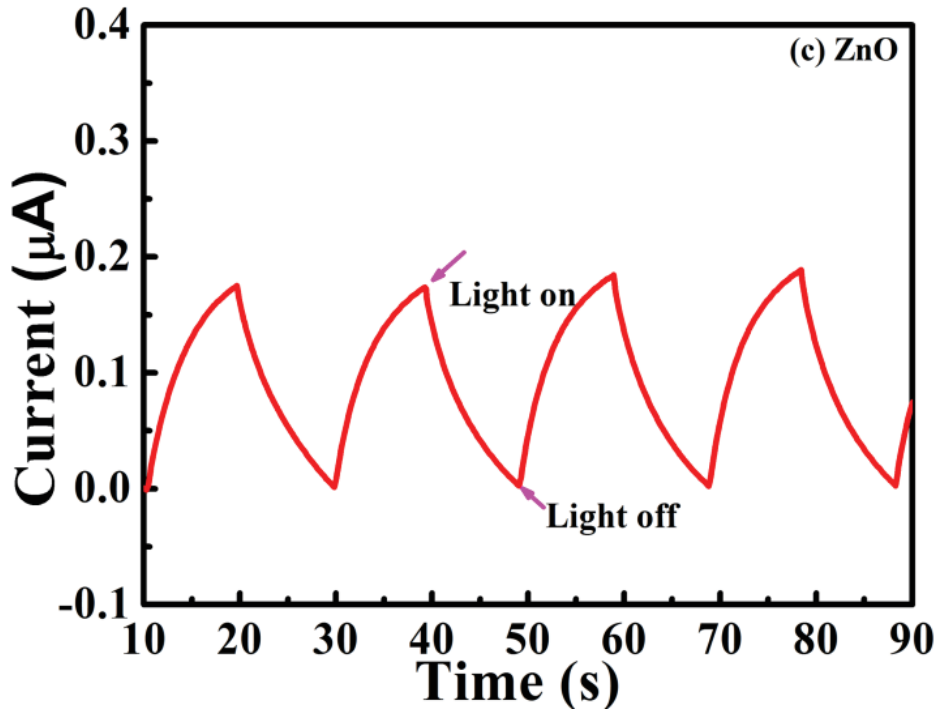


**Figure 7.5(c):** Current-Time curve of ZnO.

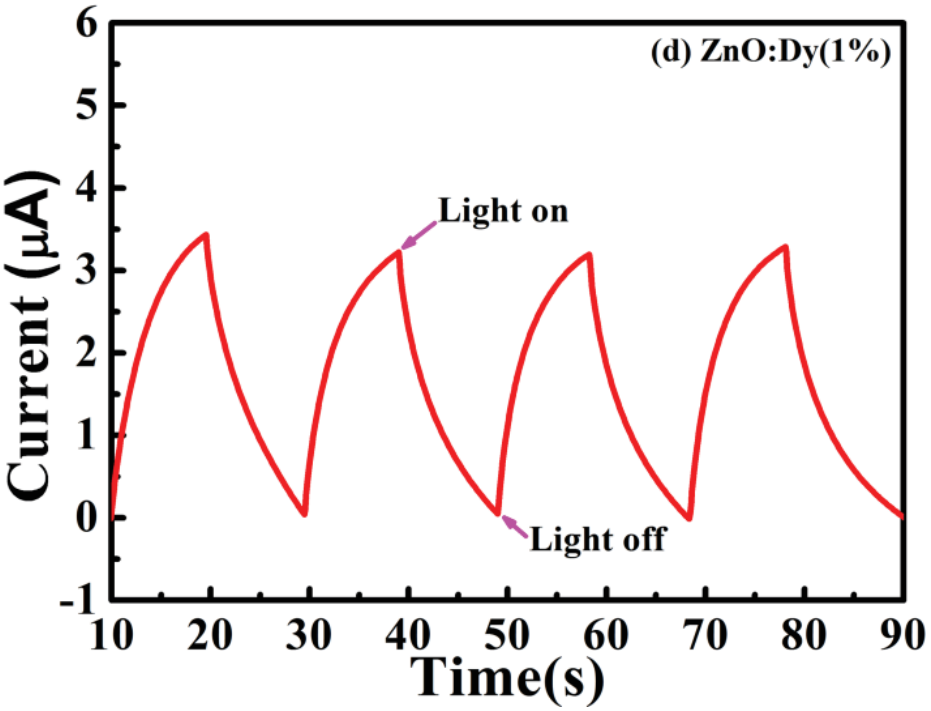


**Figure 7.5(d):** Current-Time curve of Dy doped ZnO.

### 7.4. STUDY ON COBALT DOPED ZnO THIN FILM

This study describes the effect of cobalt doping on structural optical properties of ZnO thin film. The thin film of ZnO/doped ZnO shows slightly less variation in optical and magnetic properties as compared to nanoparticles of same materials. Transition metal doped ZnO thin film have been reported for different applications such as visible light photo catalyst, gas sensor and UV photo detector [215-216].The ZnO thin film can be prepared with different method such as sputtering, pulsed laser deposition (PLD), chemical vapour deposition (CVD), spin coating, thermal evaporation, dip coating. The preparation method affects the quality of film, which influences the optical and magnetic properties of thin film. The sol-gel spin coating method has some merits, such as easy control of chemical components and fabrication of thin film at low cost to investigate structure and optical property of ZnO thin films. In this work, we have used the spin coating method for fabrication of thin film and focussed on maintaining crystalline structure to investigate its structural and optical properties.

## 7.5. RESULTS AND DISCUSSIONS OF Co DOPED ZnO THIN FILM

### 7.5.1 Structural Analysis

Figure 7.6 depicts the XRD spectra of pure and Co-doped ZnO thin film deposited on glass substrates. The sharp and intense peaks indicate the crystalline nature of samples. The observed peaks are indexed according to hexagonal wurtzite crystal structure of pure ZnO nanoparticles (PDF: 792205). The prominent peaks of ZnO [(100),(002) and (101)] are present in pure and doped samples, which confirms the hexagonal wurtzite type structure of ZnO. All the peaks of pure ZnO thin film are also present in Co-doped ZnO thin film. The XRD analysis confirms that cobalt behaves as a substitutional dopant in the ZnO and does not change the wurtzite crystal structure. The crystalline size of samples has been calculated corresponding to (002) peak using Scherer's formula (Equation 3.1). The FWHM has been calculated for (002) peaks of samples. The calculated crystallite size of ZnO and Co doped ZnO are 24nm and 26.5nm respectively. The crystallite size variation is affected by growth of ZnO grains, which depends on movement and diffusion of $Zn^{+2}$ ions. However, in case of cobalt doped ZnO, The cobalt act as electrical doping. The incorporation of cobalt increases the impurity/charge carriers and electrical conductivity because it can diffuse. Thus the grain size increases due to Co doping in the ZnO thin film.

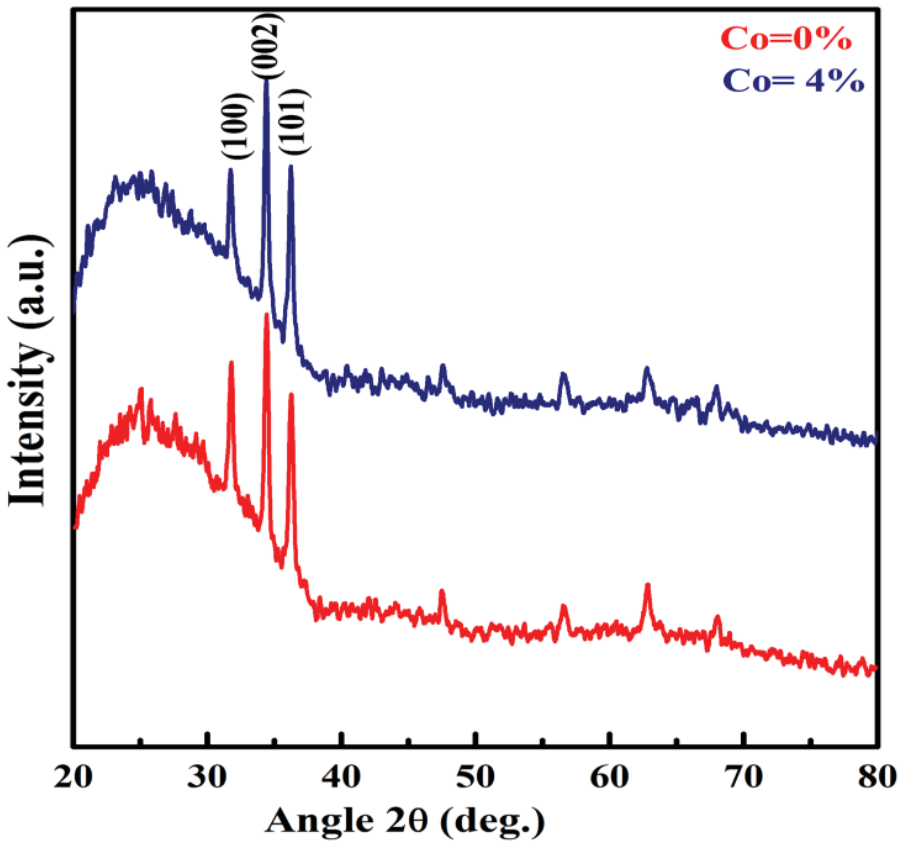


**Figure 7.6:** XRD spectra of pure and Co doped ZnO thin films.

### 7.5.2 Surface Morphology

The surface morphology of the thin films has been obtained by AFM image analysis with the help of Nova PX software. The morphology of sample does not significantly affect by Co doping. Figure 7.7(a) and (b) shows the 2d and 3d AFM image of pure ZnO thin film and indicate that deposited films are indeed continuous and of polycrystalline nature. The 2D AFM image of Co-doped ZnO thin film used for grain size calculation are depicted in Figure 7.8 AFM observations indicate a smooth surface morphology with small grains. Average grain size and roughness of cobalt doped thin film is 20.3 nm and 2.66 nm, while ZnO thin film has average grain size 30.7 nm and roughness 3.84 which indicate that cobalt doping decrease the average grain size and roughness of ZnO thin film. The small value of roughness indicates smooth surface morphology of samples.

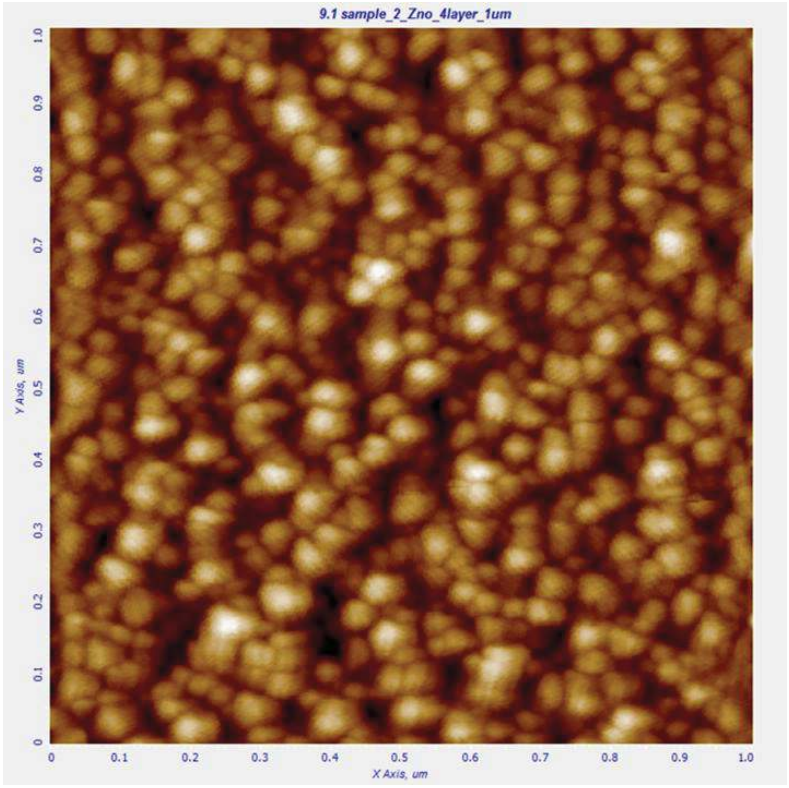


**Figure 7.7(a):** 2D AFM image of ZnO thin film.

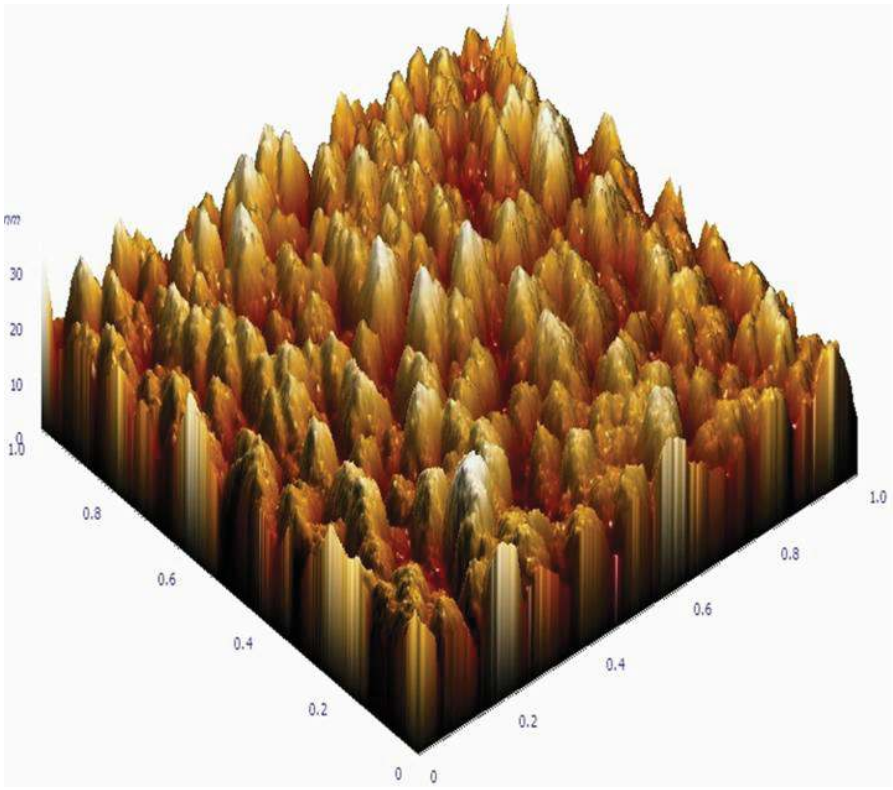


**Figure 7.7(b):** 3D AFM image of ZnO thin film.

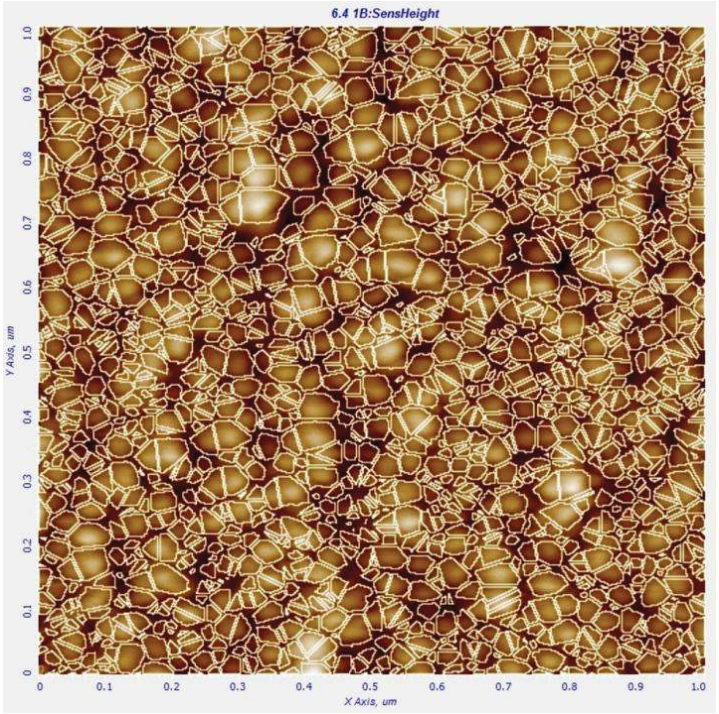


**Figure 7.8:** 2D AFM image of Co doped ZnO thin film with grain boundaries.

### 7.5.3 Thickness Measurement of the Thin Film

We have measured the thickness of thin film with the help of M-Probe measurement system. We have taken the observation at the different position of the film and average thickness has been calculated using these data. It has been observed that average thickness of samples lies in the range of 25-30 nm.

### 7.5.4 UV-Vis spectroscopy

The absorption study of thin films have been carried out using UV-Vis analysis The absorption spectra measured in the range of 300-800 nm are shown in Figure 7.9. It can be pointed out that cobalt doping results encroachment in the visible region with a red shift in band edge. The additional peaks in the range of 550nm to 720nm have been observed in Co-doped ZnO thin film. Inset of Figure 7.9 indicate close inspection in that range. Three additional peaks of Co-doped ZnO has been observed at 565nm, 610nm and 655nm can be attributed to d-d transition of tetrahedral coordinates $Co^{+2}$ ions in ZnO hexagonal wurtzite crystal structure. These peaks correspond to $^4A_2(^4F) \rightarrow {}^4A_1(^4G)$,

$^4A_2(^4F) \rightarrow {}^4T_1(^4P)$ and $^4A_2(^4F) \rightarrow {}^2E(^2G)$ transitions [106]. These peaks have been observed with significant intensity in Co-doped ZnO nanoparticles [142]. The additional peaks indicate the presence of Co in the ZnO host lattice. The Tauc relationship (Equation 3.2) has been used to calculate the band gap of samples. Tauc plot for Pure and Co-doped ZnO thin film is shown in Figure 7.10(a) and (b) respectively. We found the decrease in band gap due to Co doping. The band gap of pure ZnO thin film is 3.25eV, while for Co-doped ZnO it is 3.21eV. The observed small red shift in the band gap energy may be due to sp-d exchange interaction between ZnO band and electrons and localised *d* electron (moments) of doped Co ions. The cobalt doping causes an increase in charge carriers that affect the sp-d exchange interaction and results a red shift in the band gap. The band gap decrease due to cobalt doping has also been observed in Co-doped ZnO nanoparticles [142]. The decrease in absorption intensity in the UV region indicates that Co doped ZnO is not suitable for UV detector application.

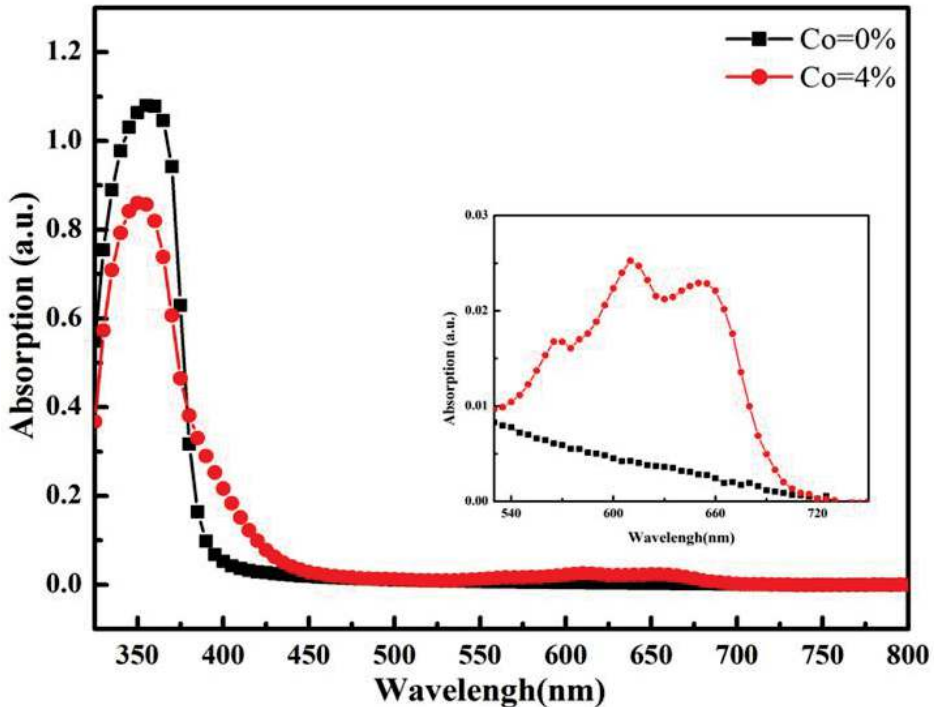


**Figure 7.9:** Absorption spectra of pure and Co doped ZnO thin films. Inset shows close inspection in the visible region.

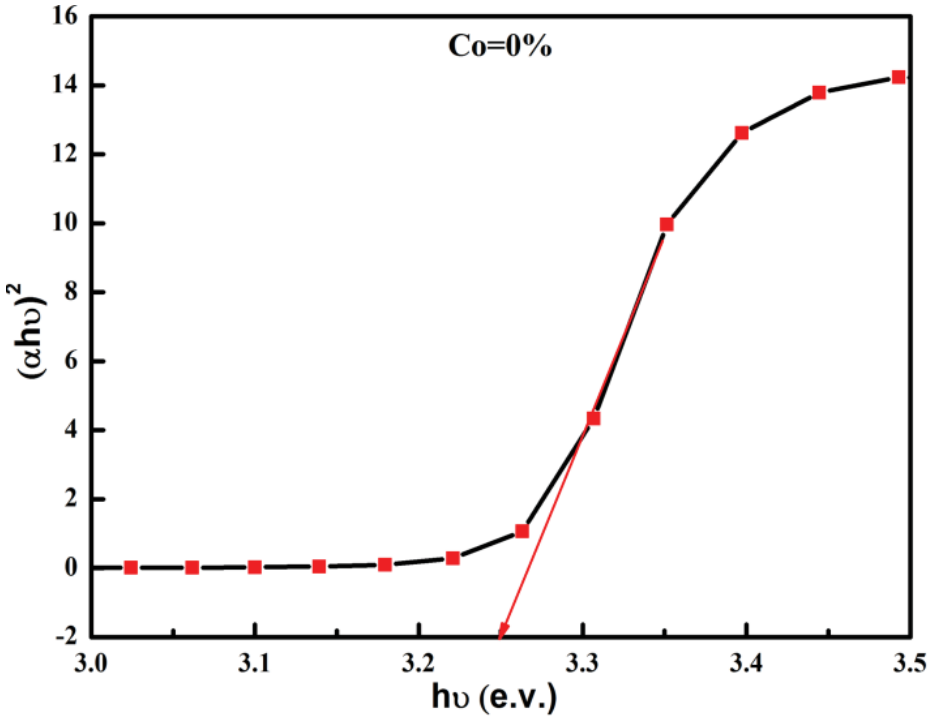


**Figure 7.10(a):** Tauc plot of ZnO thin film.

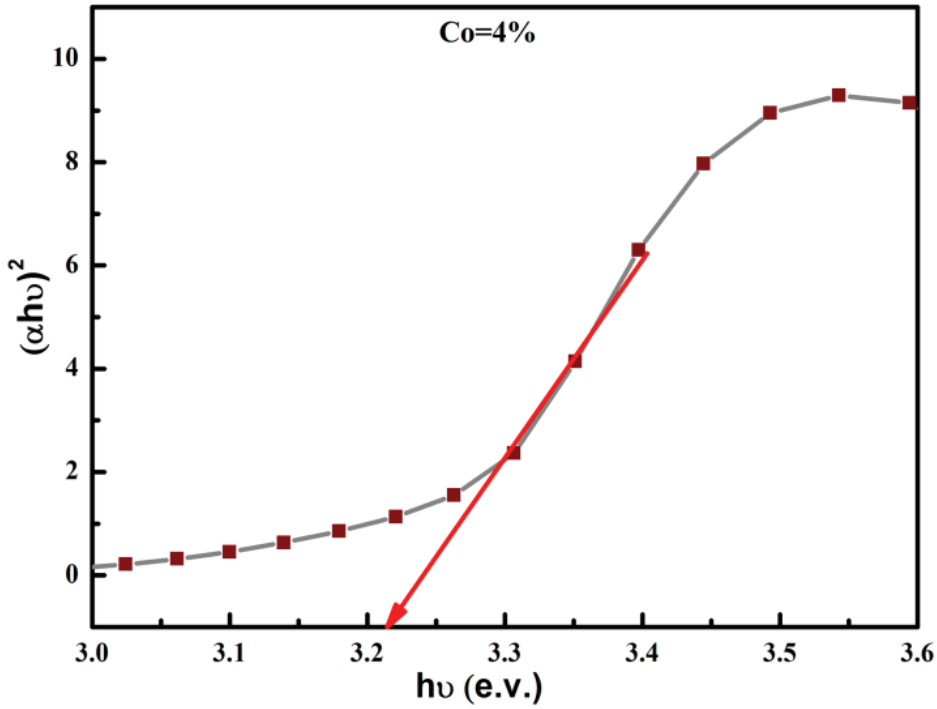


**Figure 7.10(b):** Tauc plot of Co doped ZnO thin film.

### 7.5.5 Photoluminescence Spectroscopy

The room temperature photoluminescence (PL) spectra of pure and cobalt doped ZnO thin films are shown in Figure 7.11. ZnO shows emission in the visible region (370-425nm) with a prominent peak in violet colour (389 nm), while cobalt doped ZnO sample has intense peak around 400nm with emission range 370-470nm. The observation indicates that Co doping slightly shifts the intense peak position of ZnO. We have also observed a small peak at 525nm (green colour). The peaks observed at 389nm, 400nm can be attributed to near band edge emission (NBE). The recombination of the excited electron from a localised level below the conduction band with the hole in the valence band is responsible for NBE emission. The intensity of NBE emission increases due to Co doping. This intensity enhancement can be attributed to increase in charge carriers in the system due to Co doping which favour the charge recombination process. The observed weak intensity green emission at 525 nm can be attributed to recombination of the electron with hole trapped in singly ionised oxygen vacancies.

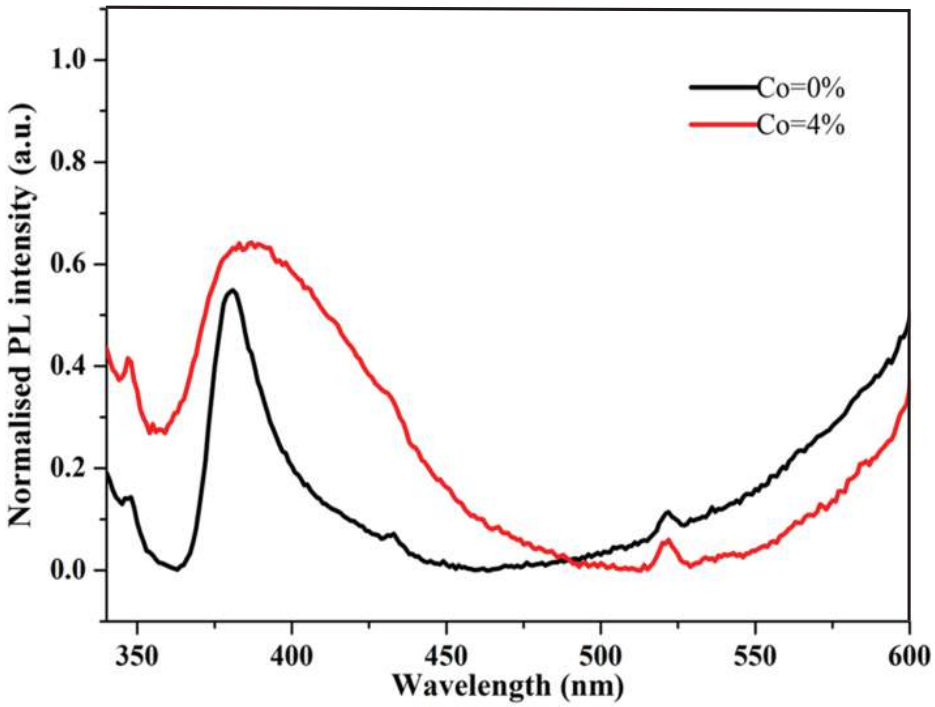


**Figure 7.11:** Photoluminescence spectra of pure and Co doped ZnO thin films.

## 7.6. CONCLUSION

In summary, the structural property, surface morphology, optical and electrical properties of ZnO and doped ZnO thin film have been investigated for its promising application in ZnO based UV detector. The thin films prepared by easy root of synthesis exhibit good crystalline quality, proper grain growth and small values of roughness. UV-Vis absorption study indicates that the absorption in the UV region increases remarkably due Dy doping in ZnO thin film. The photocurrent and responsivity of ZnO:Dy(1%) increases significantly as compared to pure ZnO. The enhance UV absorption, and high value of photocurrent in Dy doped ZnO may be attributed to enhancement in electron concentration and defects in the system, which support the sensing property of ZnO thin film.

In Co doped ZnO, we have prepared pure and Co-doped ZnO thin film and focussed on maintaining the crystalline quality of samples. The results of XRD indicate that all sample exhibit hexagonal crystalline structure. The AFM analysis ascertains smooth surface and formation of grains of approximately uniform size. The absorption study shows that Co concentration causes the occurrence of visible light absorption in the range 540-700 nm and encroachment of band edge in the visible region. The red shift in the band gap of samples has been observed due to Co doping. The photoluminescence study confirms the wide absorption visible range. The decrease in absorption intensity in the UV region indicates that Co doped ZnO is not suitable for UV detector application. However, the obtained modification in optical properties of ZnO can be useful for ZnO based optoelectronics devices.

*CHAPTER 8*

# SUMMARY AND CONCLUSIONS

In the present thesis, the effect of transition metal and rare earth doping in zinc oxide have been studied with the help of different characterisation techniques. The prepared samples have been maintained in low dimensional states to improve the optical and magnetic properties for optoelectronic and spintronics applications. Moreover, the thin film sample has been characterised for ZnO based UV detector. The important points of the thesis can be summarised as-

1. The study of structural and local structural change due to transition metal and rare earth doping in ZnO nanoparticles have been carried out via different characterisation techniques. We are focused to maintain the crystalline structure of zinc oxide.

2. The study of transition metal doped ZnO stabilizes the correlation between structural, optical and magnetic properties of ZnO, which can be useful for DMS application.

3. The investigation on enhancement of optical absorption, emission and RTFM properties of Transition metal and rare earth doped ZnO has been carried out for potential application in optoelectronics and spintronics devices.

4. To study the rare earth (Eu and Tb) doped ZnO with small doping concentration to maintain the crystalline structure and enhancement in optical emission as well as change in absorption and RTFM properties of ZnO nanoparticles with charge compensation mechanism.

5. The fabrication of doped ZnO thin film with sol gel spin coating method has been carried out to enhance UV detection performance.

Chapter wise summary of studied composition is explained as follows.

**Chapter 3:** In this chapter, we have investigated the consequences of cobalt (Co) incorporation with different doping concentrations (0, 2, 4 and 6%) on structural, optical and

magnetic properties of ZnO nanoparticles. The results of XRD, TEM, SAED pattern of single particle, EDS and FTIR authenticate the substitution of cobalt and hexagonal crystal structure without any secondary phase formation of all the samples under investigation. The UV-Vis absorption study indicates that increase in Co concentration improves the visible region absorption (550-700 nm). The absorption edge of Co doped ZnO shift towards visible region with increase in Co concentration. The band gap of samples shows a red shift with increase in Co percentage. The photoluminescence study of the samples indicates that Co doping shift the intense peak position of ZnO from violet to blue colour. The weak emission peak at 572 nm also observed in all the samples. The emission is represented by chromaticity diagram. The room temperature magnetisation curve shows that an increase of Co concentration increases the linear behaviour of M-H loop. The magnetic susceptibility results indicate that all the samples have curie- weiss behaviour. The coercive field ($H_c$) and the remanence magnetisation ($M_r$) increases with Co doping concentration.

**Chapter 4:** In this chapter, we have studied the structural, optical and magnetic properties of Mn doped ZnO nanoparticles with different doping concentrations (0, 2, 4 and 6 %) synthesized by sol gel method. Lattice parameters, cell volume, atomic packing fraction, crystallite size and confirmation of hexagonal wurtzite crystal structure have been studied by XRD data. Surface morphology as well as grain size and presence of all the elements have been confirmed by SEM and EDS respectively. The decrease in lattice parameters ratio (c/a) with Mn concentration indicates lattice distortion with the incorporation of $Mn^{2+}$ ions at $Zn^{2+}$ site of ZnO structure, which has been confirmed by Raman analysis. It has been observed that microstructure defects induced some extra Raman vibration modes. Ultraviolet-Visible analysis shows that absorption edge lies in visible region and encroachment in visible region increases while energy band gap decreases with the

increase of Mn concentrations. We have recorded FTIR spectra at room temperature to study the vibrational bands present in $Zn_{1-x}Mn_xO$ samples. The magnetic study of samples indicates ferromagnetic behaviour at room temperature. The magnetic properties increases with doping concentration due to small lattice distortion and defects.

**Chapter 5:** This chapter demonstrate the influence of different lithium concentrations (0.25-1.0%) on Eu(1%) doped zinc oxide nanoparticles synthesized by sol gel method. The results of XRD, TEM, EDS, FTIR and Raman analysis authenticate the crystalline structure and incorporation of europium and lithium in hexagonal crystal structure of zinc oxide without any impurity phase. The XPS spectra of lithium confirm the existence of Li substitutional and Li interstitial. The local structure has been investigated by X-ray absorption spectroscopy analysis. The results ascertain oxidation state of elements in samples. The variation in bond length observed by EXAFS fitting supports XPS data and indicates the presence of dopant in the host. The position of Li plays an important role in defect mediated ferromagnetism of zinc oxide. The photoluminescence study demonstrates the enhancement in europium related peak for small lithium concentration. We found that the ferromagnetism in zinc oxide reduces after europium doping, while incorporation of lithium (0.5-1.0%) in europium doped zinc oxide significantly enhances the ferromagnetic property of zinc oxide. Li substitutions contribute to ferromagnetic property of zinc oxide by stabilizing Zn vacancy and other magnetic defects. The existence of enhanced luminescence coupled with RTFM makes this material suitable for optoelectronics devices.

**Chapter 6:** The present study has been conducted to investigate the role of Li concentration (0.25-1.0%) on structural, optical and magnetic properties of sol-gel derived Tb (1%) doped zinc oxide nanoparticles. The structural analysis has been carried with the help of XRD, Raman and FTIR to ensure the crystalline structure of the samples

without any impurity phase. The local structure has been examined by XAS analysis. The variation in bond length and disorder confirm the substitution of Tb and Li in ZnO lattice. The result of XPS and XANES ascertain the oxidation state of all elements in the sample. The XPS result confirms the presence Li in the sample. The morphology and particle size are calculated by TEM characterisation. The absorption study demonstrates encroachment in the visible region up to 600nm with the incorporation of Li1.0% in Tb-doped zinc oxide. The photoluminescence analysis demonstrates the enhancement in Tb related peak with Li (0.5%) co-doping concentration. Magnetic measurement indicates the weak ferromagnetic behaviour in doped ZnO samples, while pure zinc oxide shows small diamagnetic response with a contribution of ferromagnetism. The non-magnetic lithium ions stabilize the cation vacancies and support the magnetic nature of terbium.

**Chapter 7:** In this chapter, Dy doped ZnO thin film deposited by spin coating method has been studied for its potential application in ZnO based UV detector. The investigations on the structural property and surface morphology of the thin film ensure that the prepared samples are crystalline and exhibit hexagonal crystal structure of ZnO. The small change in crystallite size has been observed due to Dy doing in ZnO. AFM analysis ascertains the grain growth and smooth surface of the thin films. The Dy doped ZnO thin film exhibit the significant enhancement in UV region absorption as compared to pure ZnO thin film, which suggests that Dy doped ZnO can be used as a UV detector. Under UV irradiation of wavelength 325nm, the photocurrent value of Dy doped ZnO is 105.54μA at 4.5 V, which is 31 times greater than un-doped ZnO thin film (3.39 μA). The calculated value of responsivity is found to increase significantly due to the incorporation of Dy in the ZnO lattice. The observed higher value of photocurrent and responsivity could be attributed to the substitution of Dy in ZnO lattice, which enhances the conductivity, electron mobility, defects in ZnO and benefit the UV sensing property.

Further, we have investigated the effect of Co(4%) doping on structural and optical properties of the zinc oxides thin film deposited on glass substrate by spin coating techniques. The structural analysis and surface morphology have been carried out with the help of XRD and AFM characterisation respectively. UV-Vis spectroscopy and Photoluminescence spectroscopy has been employed to obtain information about absorption and luminescence properties of pure and Co-doped ZnO thin film. The XRD patterns confirm the crystalline nature and hexagonal wurtzite structure formation in the samples. The thickness of the film is measured by MProbe Thin Film Measurement System. AFM observations indicate a smooth surface morphology with small grains. AFM results suggest that cobalt doping decreases the average grain size and roughness of ZnO thin film. UV-Vis analysis indicates that absorption edge of cobalt doped ZnO thin film lie in the visible region and energy band gap of $Zn_{0.96}Co_{0.04}O$ (3.05eV) is less than pure ZnO thin film (3.2eV). The defect generated absorption in the visible region is present due to the incorporation of cobalt in ZnO thin film. Photoluminescence study shows the broad emission in the visible region in all samples. The Co doping causes an increase in broad emission in the visible region.

The thesis firmly empowers the investigations on structural optical and magnetic properties of transition metal and rare earth doped ZnO in low dimensional sates. The details discussion with the help of various experimental techniques provides clear insight about the factors which influences the properties of zinc oxide in low dimensional sates.